Electronic Supplementary Information

Carbonyl group-dependent high-throughput screening and enzymatic characterization of diaromatic ketone reductase

Jieyu Zhou, Guochao Xu, Ruizhi Han, Jinjun Dong, Weiguo Zhang, Rongzhen Zhang, Ye Ni*

The Key Laboratory of Industrial Biotechnology, Ministry of Education, School of Biotechnology, Jiangnan University, Wuxi 214122, Jiangsu, China

*Corresponding author. Tel/Fax: +86-510-85329265; E-mail: yni@jiangnan.edu.cn

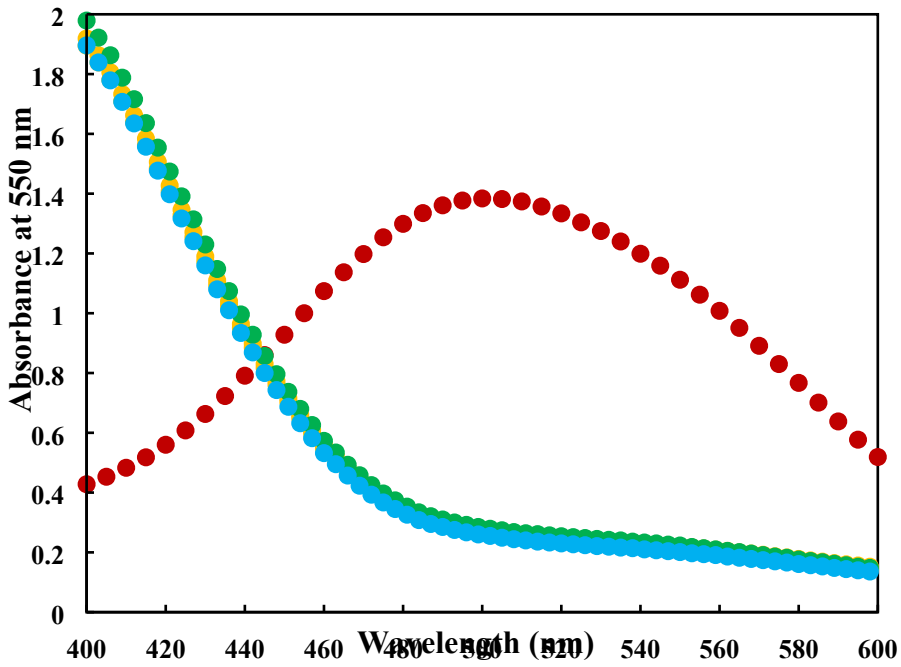

Figure S1 Absorbance spectra of CPMK (ᔓ), crude extracts of *E. coli* BL21(DE3)/pET28a (ᔓ),), *E. coli* BL21(DE3)/pET28a-*gdh* ((ᔓ),), *E. coli* BL21(DE3)/pET28a-*kpadh* ((ᔓ),) using DNPH method.

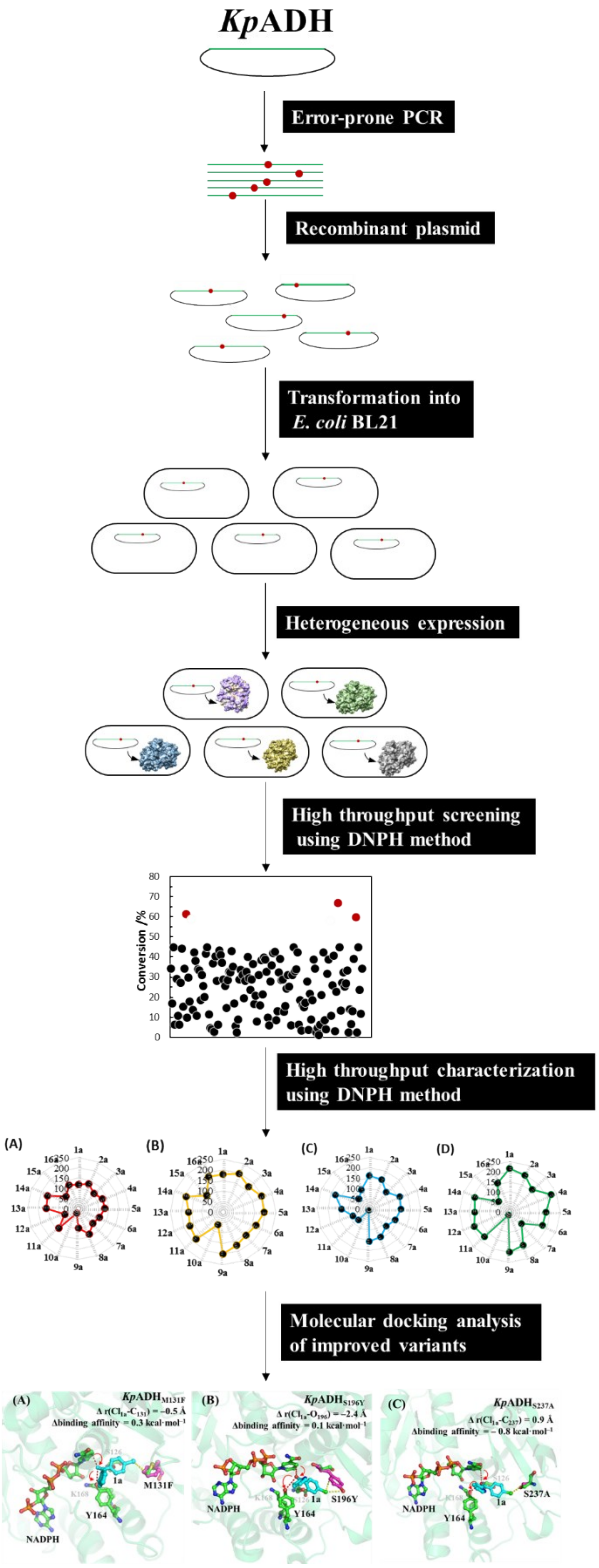

Figure S2 Flow chart of random mutagenesis, screening and characterization of *Kp*ADH variants using DNPH method.

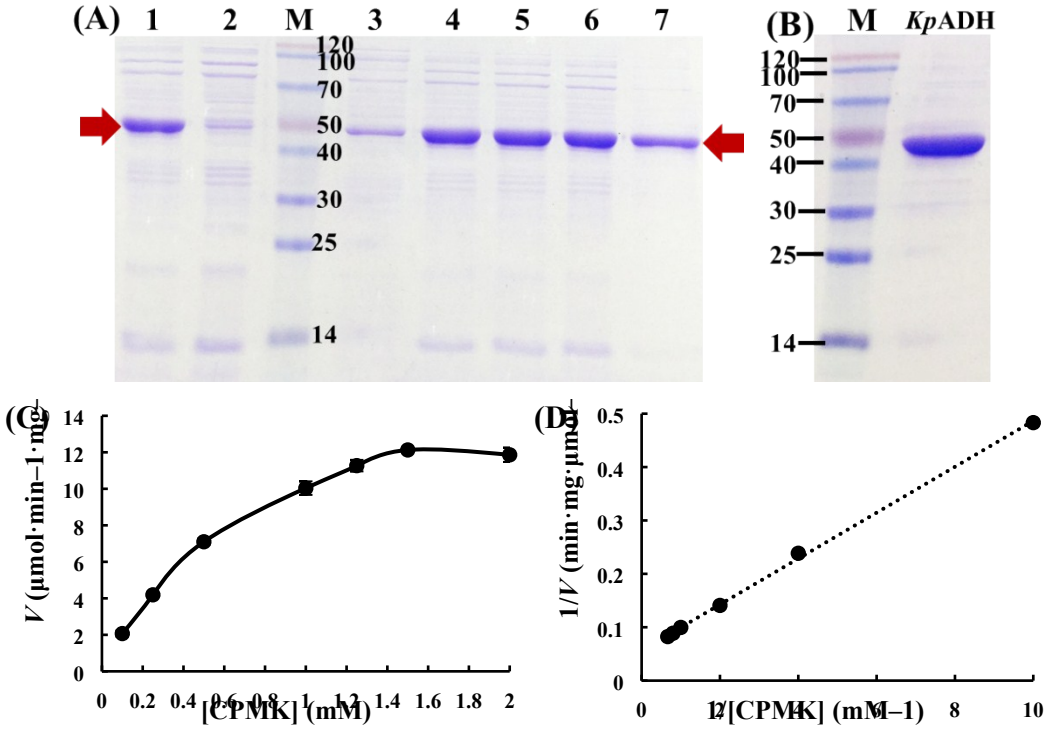

Figure S3 Purification and kinetic analysis of *Kp*ADH. (A) Purification of *Kp*ADH; lane 1: crude extract of *Kp*ADH, lane 2: flow-through of nickel column, lane 3: eluent with 50 mM imidazole, lanes 4–7: eluents with 100 mM imidazole, lane 7: eluent with 300 mM imidazole, lane M: protein molecular marker. (B) SDS-PAGE of purified *Kp*ADH. (C) Effect of CPMK concentration on the initial velocity of *Kp*ADH. (D) Lineweaver-Burk plot of *Kp*ADH.

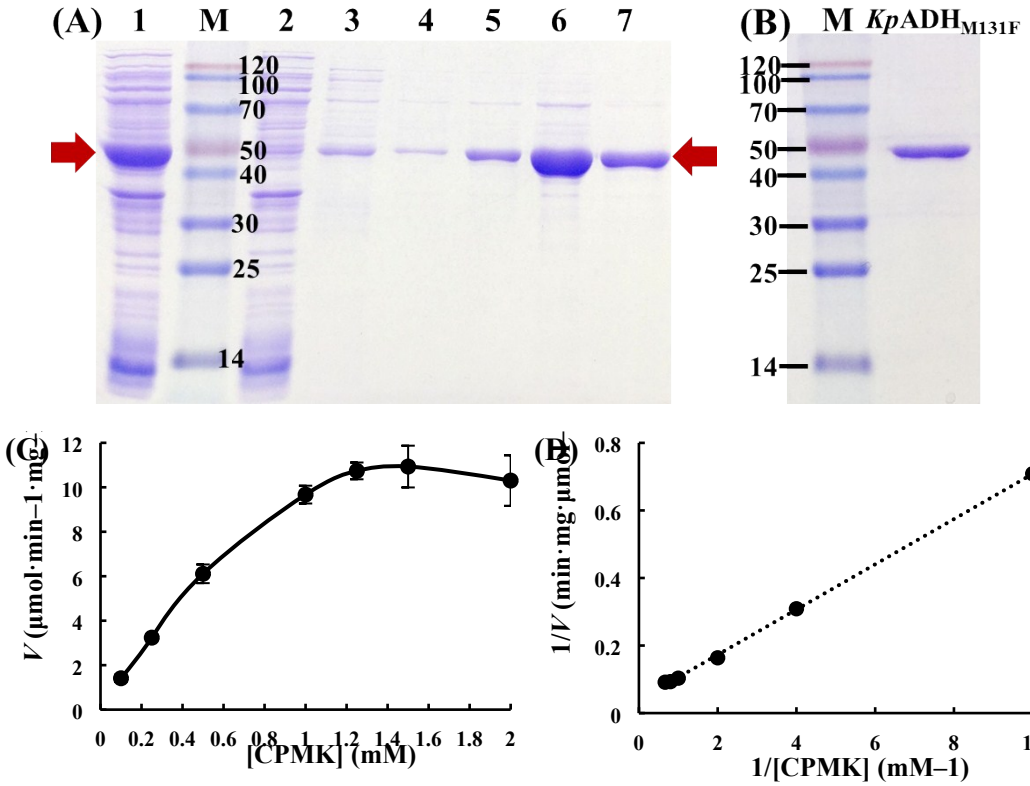

Figure S4 Purification and kinetic analysis of *Kp*ADH$_{M131F}$. (A) Purification of *Kp*ADH$_{M131F}$; lane 1: crude extract of *Kp*ADH$_{M131F}$, lane 2: flow-through of nickel column, lane 3: eluent with 50 mM imidazole, lanes 4–7: eluents with 100 mM imidazole, lane 7: eluent with 300 mM imidazole, lane M: protein molecular marker. (B) SDS-PAGE of purified *Kp*ADH$_{M131F}$. (C) Effect of CPMK concentration on the initial velocity of *Kp*ADH$_{M131F}$. (D) Lineweaver-Burk plot of *Kp*ADH$_{M131F}$.

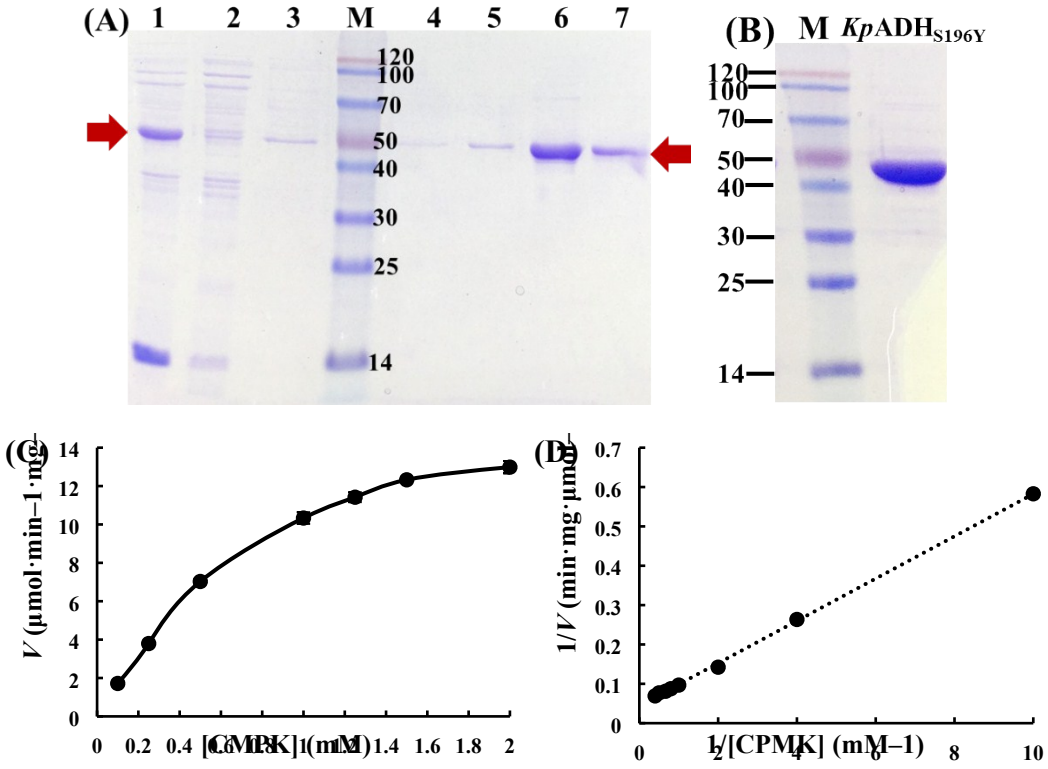

Figure S5 Purification and kinetic analysis of *Kp*ADH$_{S196Y}$. (A) Purification of *Kp*ADH$_{S196Y}$; lane 1: crude extract of *Kp*ADH$_{S196Y}$, lane 2: flow-through of nickel column, lane 3: eluent with 50 mM imidazole, lanes 4–7: eluents with 100 mM imidazole, lane 7: eluent with 300 mM imidazole, lane M: protein molecular marker. (B) SDS-PAGE of purified *Kp*ADH$_{S196Y}$. (C) Effect of CPMK concentration on the initial velocity of *Kp*ADH$_{S196Y}$. (D) Lineweaver-Burk plot of *Kp*ADH$_{S196Y}$.

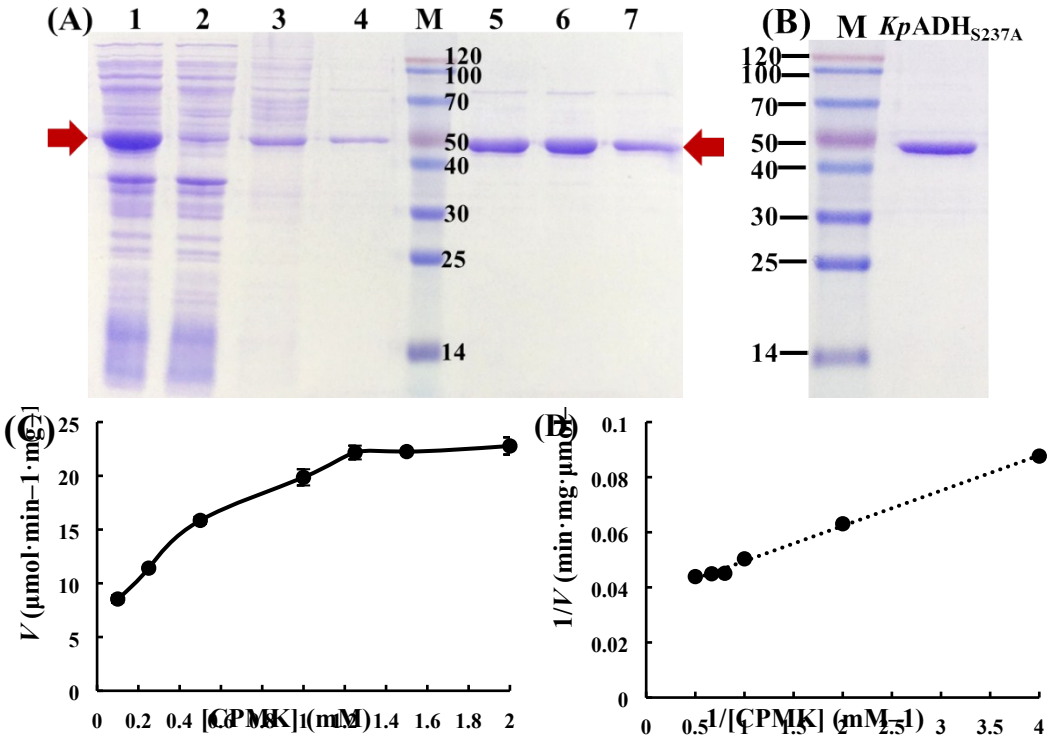

Figure S6 Purification and kinetic analysis of *Kp*ADH$_{S237A}$. (A) Purification of *Kp*ADH$_{S237A}$; lane 1: crude extract of *Kp*ADH$_{S237A}$, lane 2: flow-through of nickel column, lane 3: eluent with 50 mM imidazole, lanes 4–7: eluents with 100 mM imidazole, lane 7: eluent with 300 mM imidazole, lane M: protein molecular marker. (B) SDS-PAGE of purified *Kp*ADH$_{S237A}$. (C) Effect of CPMK concentration on the initial velocity of *Kp*ADH$_{S237A}$. (D) Lineweaver-Burk plot of *Kp*ADH$_{S237A}$.

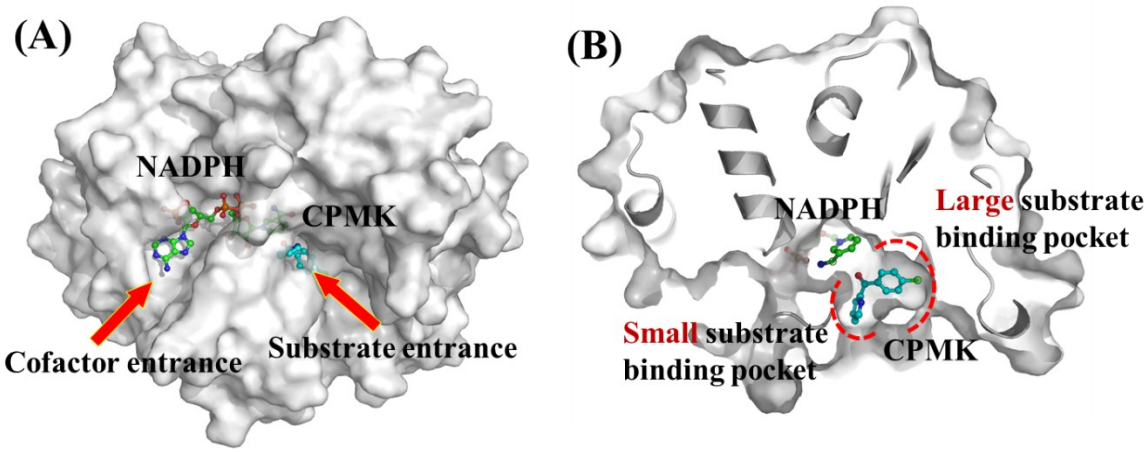

Figure S7 Homology structure of *Kp*ADH using crystal structure of yeast methylglyoxal/isovaleraldehyde reductase (PDB: 4PVC) as template. (A) Overall structure of *Kp*ADH. (B) Large and small substrate binding pockets. NADPH was depicted in green, CPMK was shown in cyan.

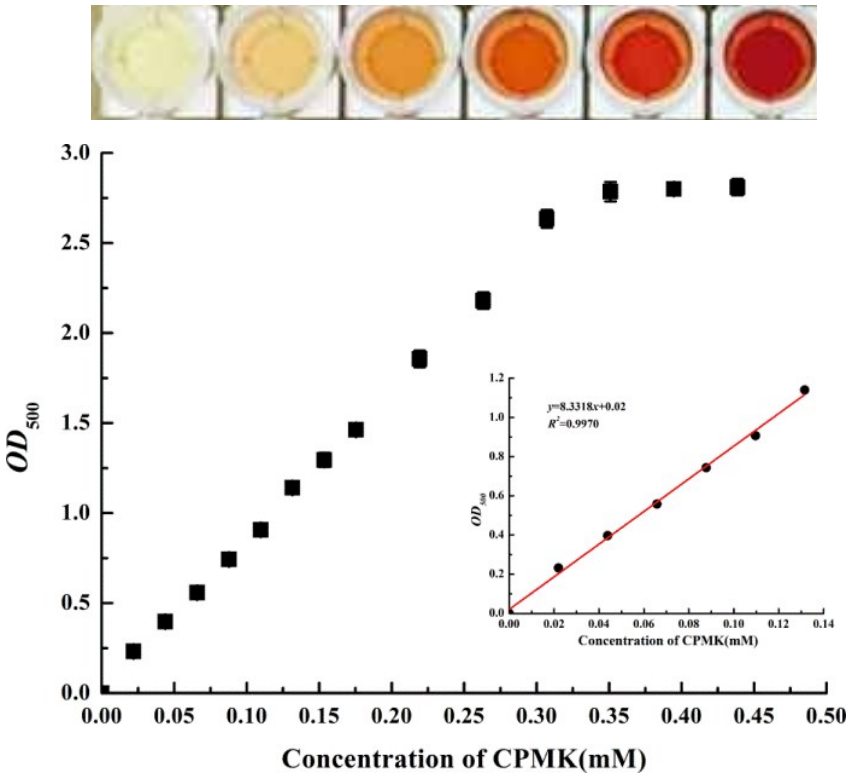

Figure S8 Absorbance at 500 nm of CPMK with different concentrations.

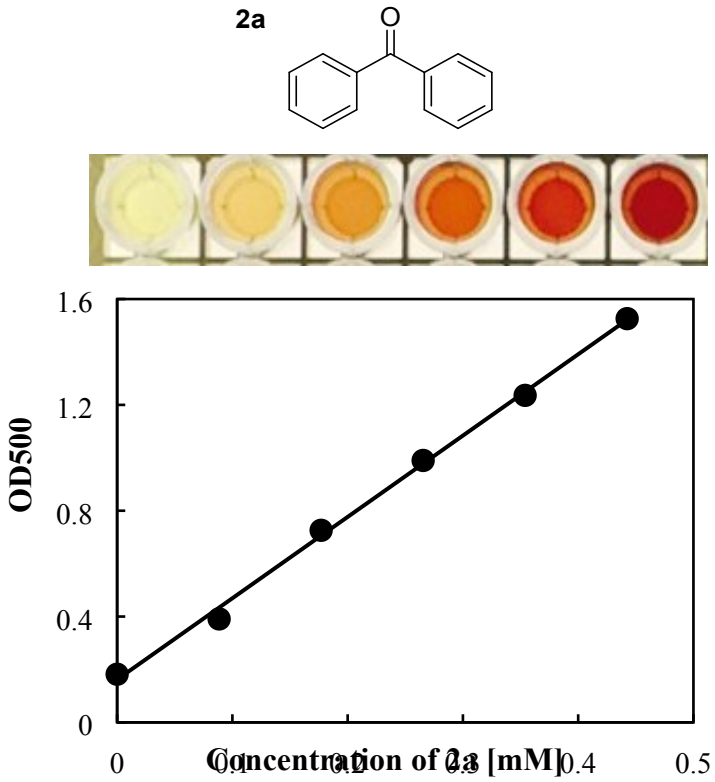

Figure S9 Standard curve of **2a** using DNPH method

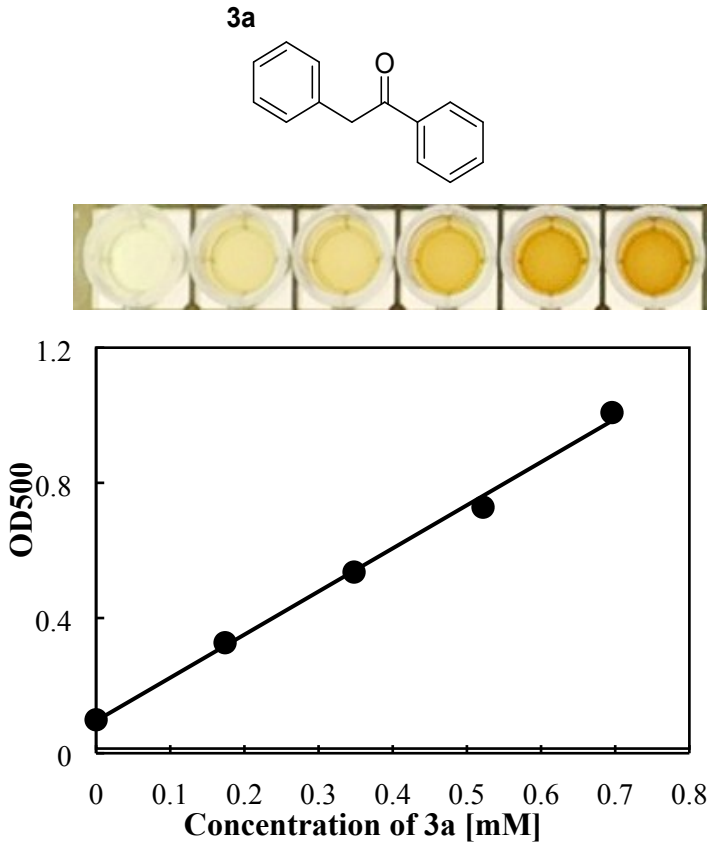

Figure S10 Standard curve of **3a** using DNPH method.

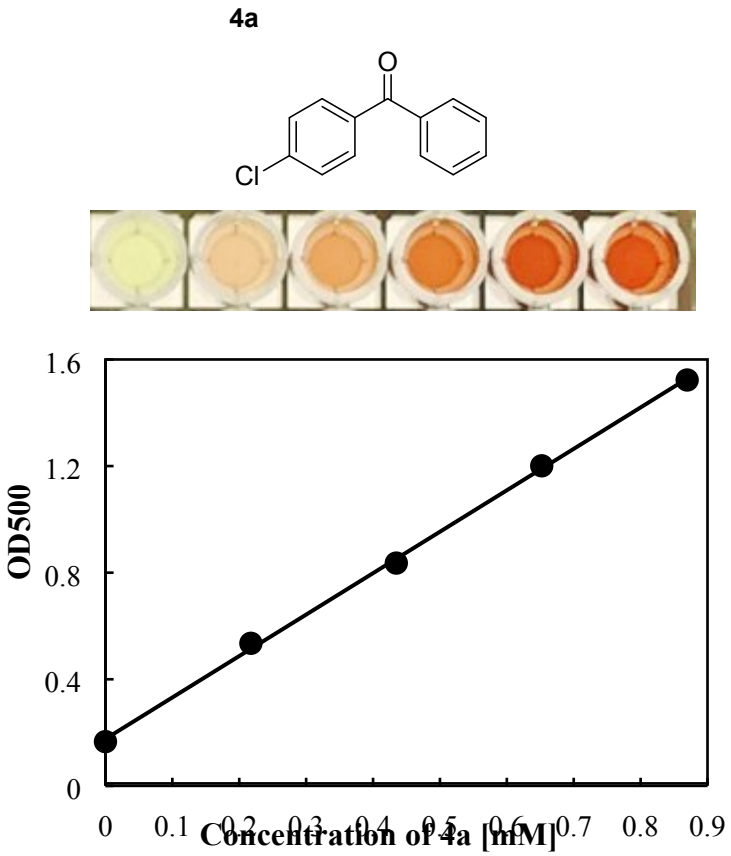

Figure S11 Standard curve of **4a** using DNPH method.

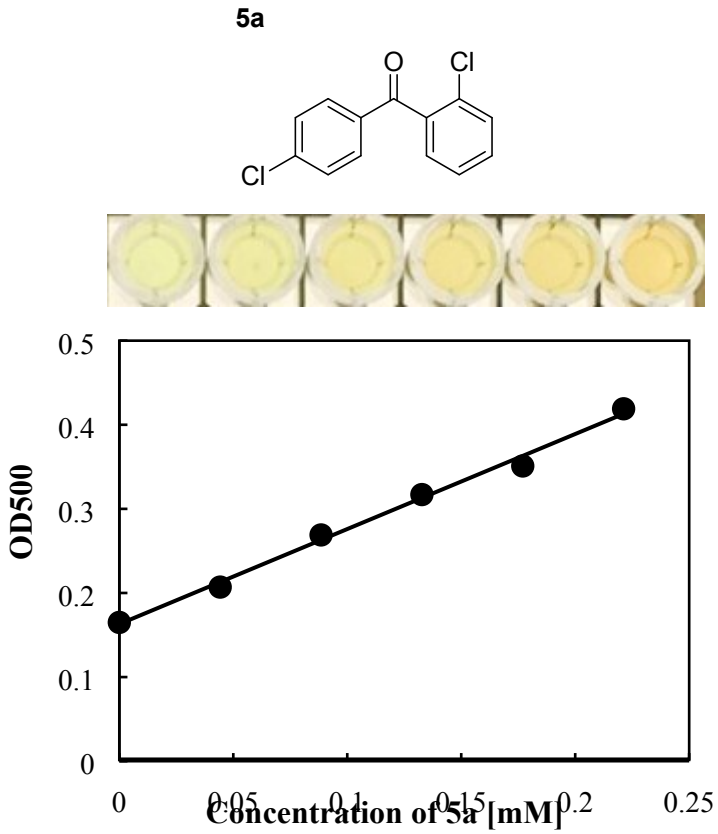

Figure S12 Standard curve of **5a** using DNPH method.

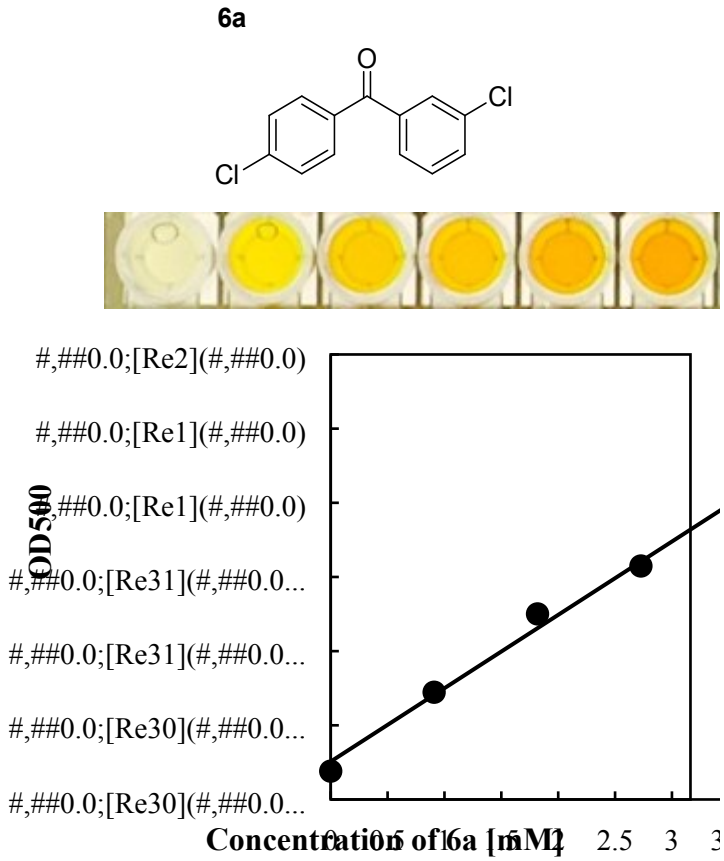

Figure S13 Standard curve of **6a** using DNPH method.

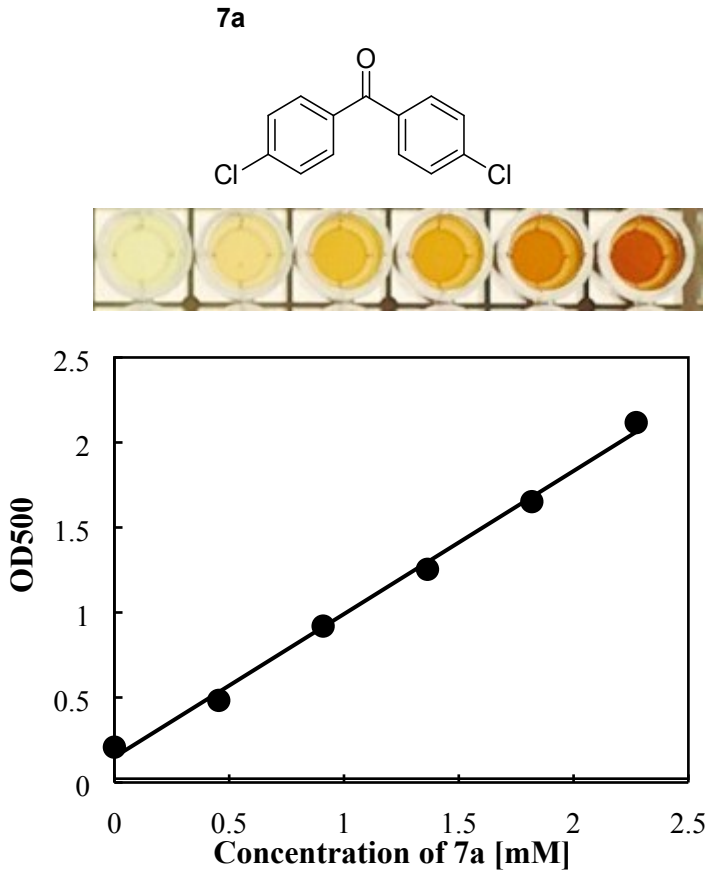

Figure S14 Standard curve of **7a** using DNPH method.

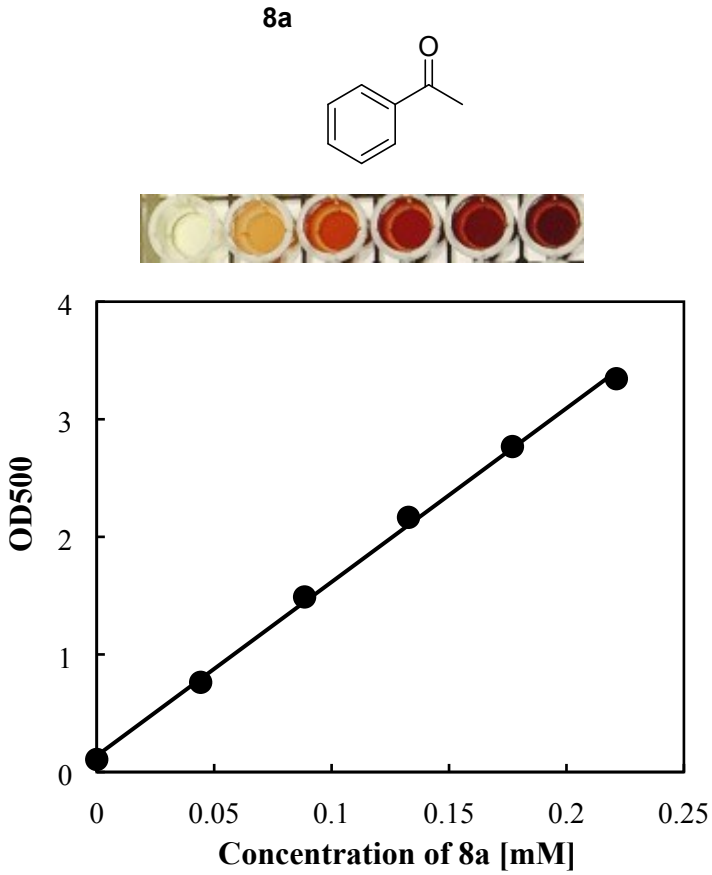

Figure S15 Standard curve of **8a** using DNPH method.

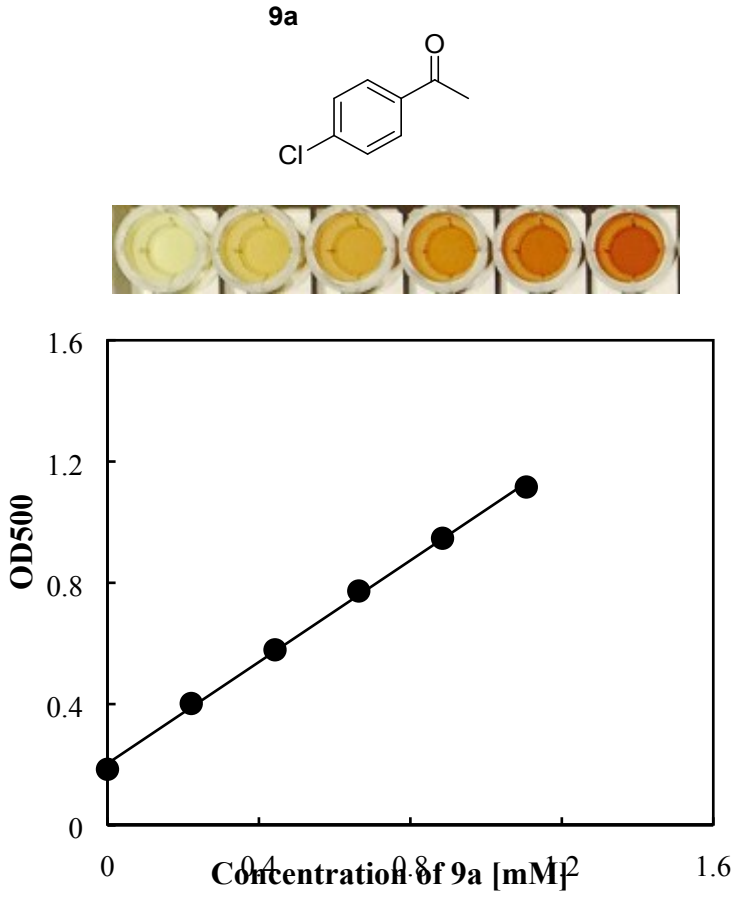

Figure S16 Standard curve of **9a** using DNPH method.

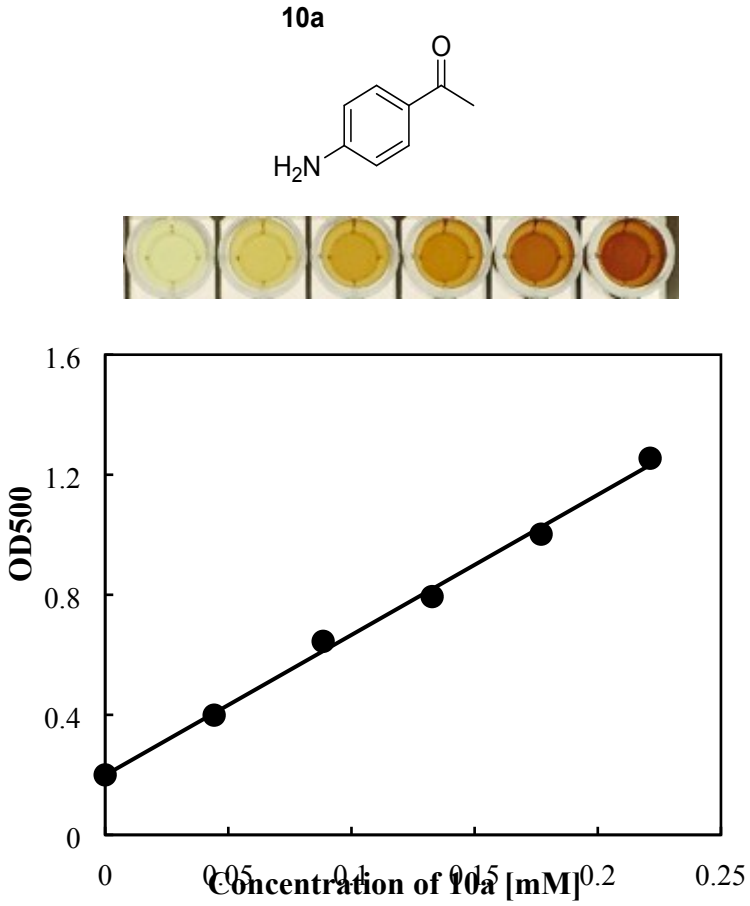

Figure S17 Standard curve of **10a** using DNPH method.

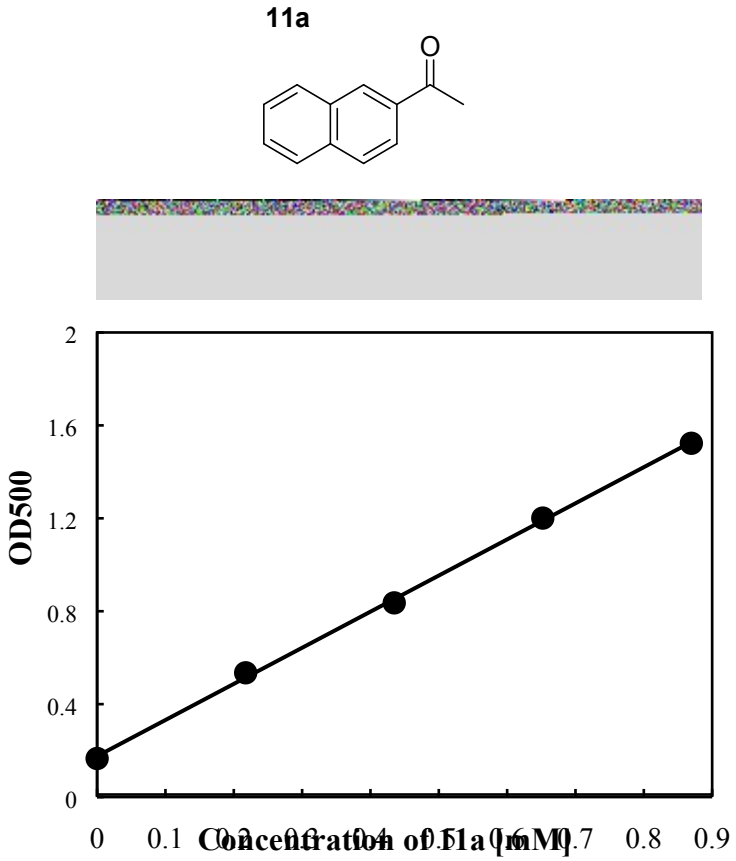

Figure S18 Standard curve of **11a** using DNPH method.

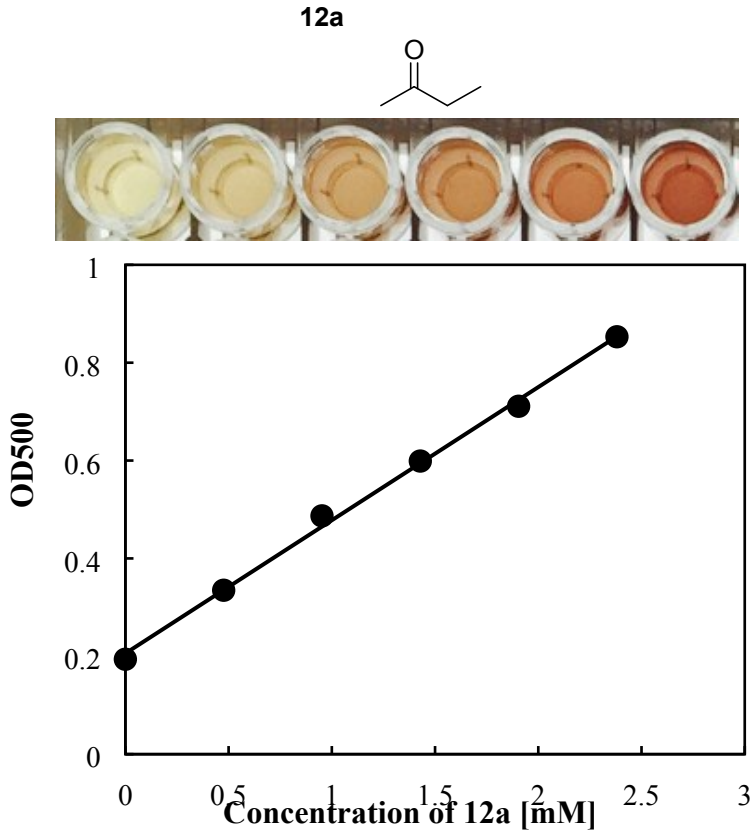

Figure S19 Standard curve of **12a** using DNPH method.

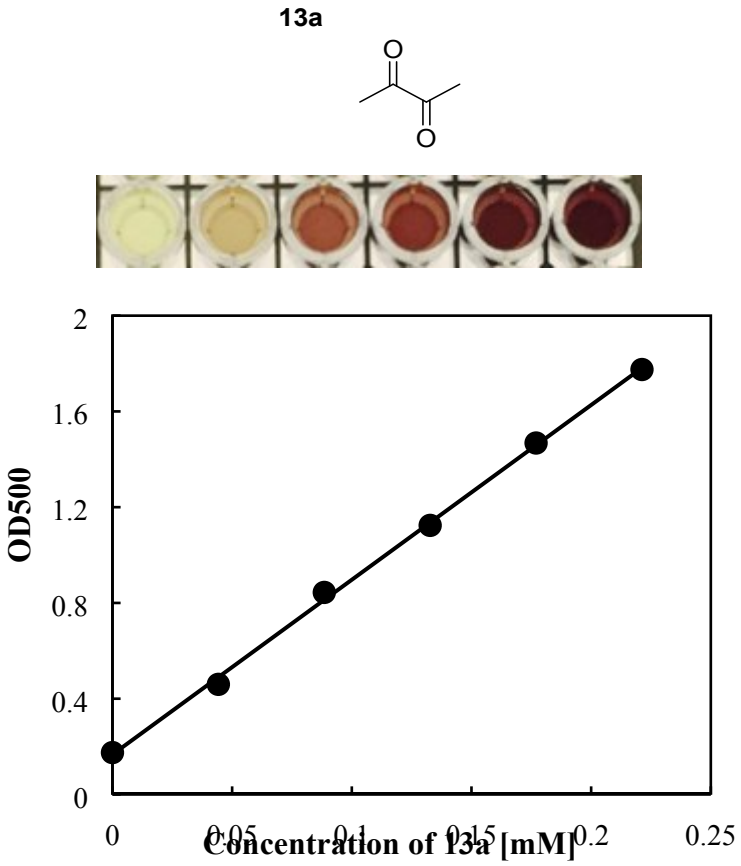

Figure S20 Standard curve of **13a** using DNPH method.

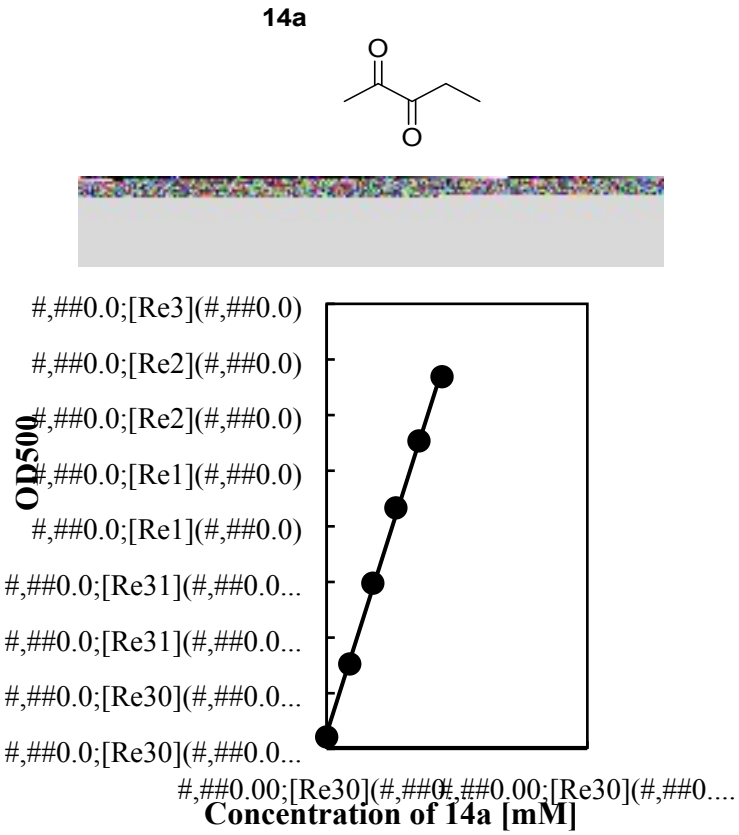

Figure S21 Standard curve of **14a** using DNPH method.

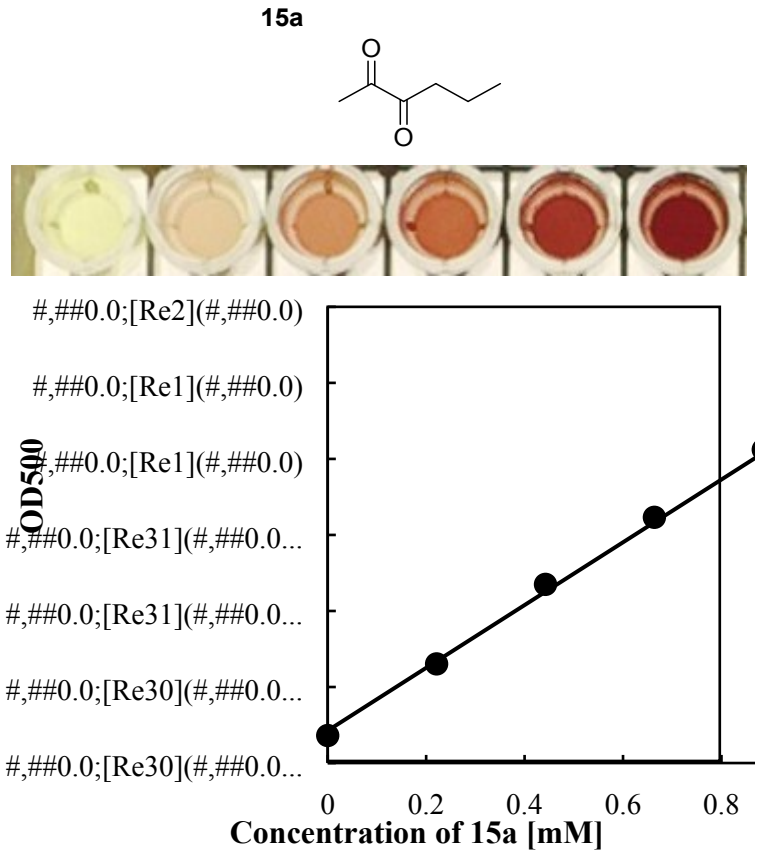

Figure S22 Standard curve of **15a** using DNPH method.

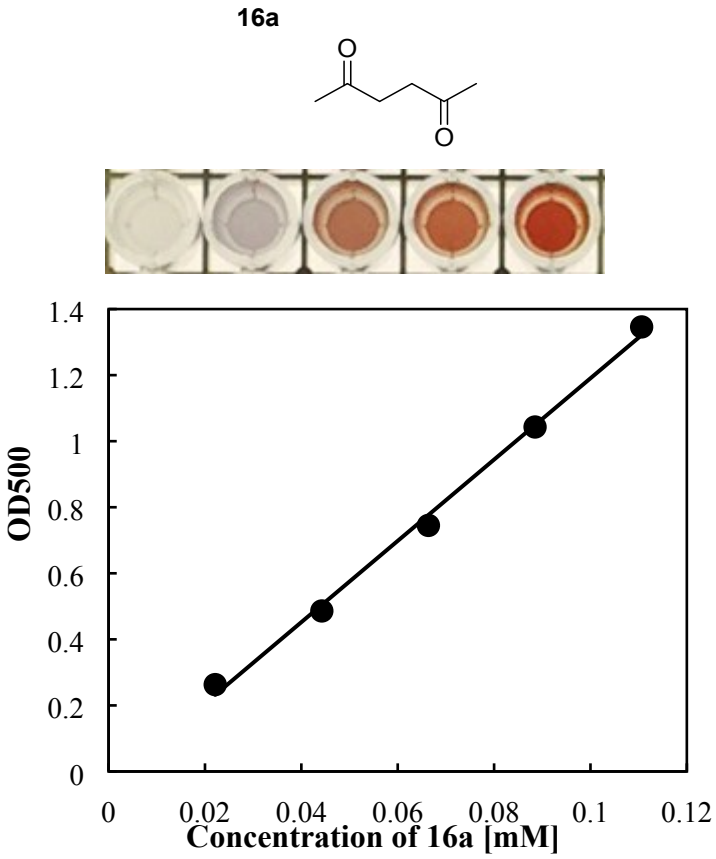

Figure S23 Standard curve of **16a** using DNPH method.

Table S1 Substrate specificities of *Kp*ADH and its variants M131F, S196A and S237A.

Substrate	*Kp*ADH [U/g wet cell]	M131F [U/g wet cell]	S196Y [U/g wet cell]	S237A [U/g wet cell]
S1	118 ± 6	181 ± 9	161 ± 8	215 ± 6
S2	131 ± 8	197 ± 5	155 ± 7	198 ± 5
S3	107 ± 6	172 ± 6	118 ± 3	158 ± 8
S4	128 ± 5	199 ± 8	159 ± 5	223 ± 6
S5	129 ± 5	194 ± 7	152 ± 4	179 ± 9
S6	111 ± 8	168 ± 8	137 ± 5	176 ± 6
S7	101 ± 5	155 ± 5	115 ± 6	83 ± 4
S8	137 ± 5	169 ± 5	144 ± 5	178 ± 6
S9	95 ± 5	198 ± 8	156 ± 5	199 ± 8
S10	23 ± 3	64 ± 3	4 ± 1	16 ± 3
S11	136 ± 6	182 ± 5	72 ± 4	175 ± 5
S12	72 ± 4	169 ± 6	84 ± 3	189 ± 6
S13	159 ± 8	164 ± 6	133 ± 7	173 ± 6
S14	163 ± 6	191 ± 5	178 ± 6	188 ± 4
S15	86 ± 4	111 ± 5	70 ± 3	75 ± 4
S16	125 ± 6	181 ± 4	100 ± 5	156 ± 3

Table S2 Conversion of *Kp*ADH, M131F, S196A and S237A toward prochiral ketones.

Substrate	*Kp*ADH [%]	M131F [%]	S196Y [%]	S237A [%]
S1	47.2 ± 2.4	72.3 ±3.6	64.6 ± 3.2	86.2 ± 2.3
S2	52.4 ± 3.0	78.7 ±2.0	61.9 ± 2.7	79.2 ± 2.0
S3	43.0 ± 2.4	68.7 ± 2.4	47.3 ± 1.4	63.2 ± 3.2
S4	51.3 ± 2.2	79.6 ± 3.2	63.6 ± 2.0	89.3 ± 2.5
S5	51.6 ± 2.0	77.4 ± 3.0	60.9 ± 1.7	71.8 ± 3.6
S6	44.5 ± 3.0	67.1 ± 3.0	54.7 ± 2.0	70.3 ± 2.5
S7	40.5 ± 2.1	62.0 ± 2.1	46.2 ± 2.6	33.2 ± 1.7
S8	54.7 ± 1.8	67.7 ± 1.5	57.6 ± 2.5	71.1 ± 1.6
S9	38.0 ± 1.2	79.1 ± 1.4	62.5 ± 3.6	79.6 ± 1.4
S10	9.3 ± 1.4	25.4 ± 2.3	1.8 ± 0.3	6.6 ± 1.4
S11	54.4 ± 2.6	72.7 ± 2.2	28.8 ± 2.3	70.2 ± 3.0
S12	29.0 ± 2.0	67.6 ± 2.0	33.5 ± 2.0	75.7 ± 2.1
S13	63.6 ± 2.2	65.4 ± 2.3	53.4 ± 1.7	69.2 ± 2.5
S14	65.4 ± 2.9	76.5 ± 1.8	71.3 ± 1.6	75.2 ± 1.5
S15	34.4 ± 2.5	44.4 ± 1.2	27.9 ± 1.4	3.4 ± 0.4
S16	50.0 ± 1.3	72.5 ± 2.6	40.0 ± 2.0	62.5 ± 2.3